5-27-2004

Seasonal Analyses of Air Pollution and Mortality in 100 U.S. Cities

Roger D. Peng
Johns Hopkins Bloomberg School of Public Health, Department of Biostatistics, rpeng@jhsph.edu

Francesca Dominici
Johns Hopkins Bloomberg School of Public Health, Department of Biostatistics, fdominic@jhsph.edu

Roberto Pastor-Barriuso
Department of Epidemiology & Biostatistics, Escuela Nacional de Sanidad, szeger@jhsph.edu

Scott L. Zeger
Johns Hopkins Bloomberg School of Public Health, Department of Biostatistics, szeger@jhsph.edu

Jonathan M. Samet
Johns Hopkins Bloomberg School of Public Health, Department of Epidemiology, cgerczak@jhsph.edu

Seasonal Analyses of Air Pollution and Mortality in 100 U.S. Cities

Roger D. Peng Francesca Dominici Roberto Pastor-Barriuso Scott L. Zeger

Jonathan M. Samet

Word count: 3547

Abstract

Time series models relating short-term changes in air pollution levels to daily mortality counts typically assume that the effects of air pollution on the log relative rate of mortality do not vary with time. However, these short-term effects might plausibly vary by season. Changes in the sources of air pollution and meteorology can result in changes in characteristics of the air pollution mixture across seasons. The authors develop Bayesian semi-parametric hierarchical models for estimating time-varying effects of pollution on mortality in multi-site time series studies. The methods are applied to the updated National Morbidity and Mortality Air Pollution Study database for the period 1987–2000, which includes data for 100 U.S. cities. At the national level, a 10 μg/m^3 increase in PM$_{10}$ at lag 1 is associated with a 0.15 (95% posterior interval: −0.08, 0.39), 0.14 (−0.14, 0.42), 0.36 (0.11, 0.61), and 0.14 (−0.06, 0.34) percent increase in mortality for winter, spring, summer, and fall, respectively. An analysis by geographical regions finds a strong seasonal pattern in the northeast (with a peak in summer) and little seasonal variation in the southern regions of the country. These results provide useful information for understanding particle toxicity and guiding future analyses of particle constituent data.

Word count: 200

MeSH headings: air pollution, epidemiology, models/statistical, mortality

Acknowledgments

This research was supported in part by NIH/NHLBI grant T32HL07024, NIEHS grant R01ES012054 and Health Effects Institute grant HEI025. Any opinions, findings, and conclusions or recommendations expressed in this material are those of the authors and do not necessarily reflect the views of these funding agencies.

Numerous time series studies have indicated a positive association between short-term variation in ambient levels of particulate matter (PM) and daily mortality counts (see e.g. 1–3). The models used in these studies have typically assumed that the association between PM and daily mortality is constant over the study interval. However, the short-term effects of PM on mortality might plausibly exhibit seasonal variation. Studies in a number of locations have shown that that the characteristics of the PM mixture change throughout the year and that the relative and absolute contributions of particular components to PM mass may be different during different times of the year (4, ch. 3 and references therein). Patterns of human activity also change from season to season, so that a particular air pollution concentration in one season may lead to a different exposure in another season. Other potential time-varying confounding and modifying factors, such as temperature and influenza epidemics, can also affect estimates of short-term effects of air pollution on mortality differently in different seasons. All of the issues described above indicate a need to extend current models for time series data on air pollution and health to incorporate time-varying pollution effects.

The composition of particulate matter is known to vary in the spatial domain as well, suggesting that seasonal patterns should be examined by geographical region (5). For example, in the North West wood burning is a greater source of PM in the colder seasons than in the warmer months. The PM mixture in the Eastern U.S. contains a large fraction of sulfates (almost 40% of total mass) originating from power plants in the Midwest, while PM in areas of the Western U.S. such as Southern California and the Pacific North West contains more nitrates and organic compounds (approximately 30% of total mass) (4–6).

In this paper we develop statistical methods for estimating seasonal patterns in the short-term effects of air pollution on mortality in multi-site time series studies. We propose Bayesian semi-parametric hierarchical models for estimating time-varying health effects within each city and for comparing temporal patterns across cities and geographical regions. Using updated data from the National Morbidity, Mortality, and Air Pollution Study (NMMAPS) (7), we estimate seasonal patterns in the short-term effects of PM less than 10 μm in aerodynamic diameter (PM_{10}) on daily non-accidental mortality in 100 U.S. cities for the period 1987–2000. These patterns are estimated for seven geographical regions and on average for the entire U.S. We explore the sensitivity of estimated seasonal patterns to temperature adjustment, copollutants, exposure lag, and adjustments for long-term mortality trends.

MATERIALS AND METHODS

The NMMAPS database contains daily time series of mortality, weather, and air pollution assembled from publicly available sources for the largest 100 cities in the United States. A full description of the construction of the database can be found in (7). The most recent data are available at `http://www.ihapss.jhsph.edu`.

Within each city, we specify a semi-parametric regression model for the time-varying log relative rate using a generalized additive model framework (8). More specifically, let Y_t^c be the total number of non-accidental deaths on day t in city c. The Y_t^c are Poisson distributed with expectation μ_t^c and with possible overdispersion ϕ^c. The general form of the city-specific model is

$$\begin{aligned} Y_t^c &\sim \text{Poisson}(\mu_t^c) \\ \text{Var}(Y_t^c) &= \phi^c \mu_t^c \\ \log(\mu_t^c) &= \beta^c(t)\, x_{t-\ell}^c + \text{confounders} \qquad (1) \end{aligned}$$

where $x_{t-\ell}^c$ is the lag ℓ PM_{10} level for day t.

The function $\beta^c(t)$ in equation 1 represents the time-varying effect of PM_{10} on mortality and is a yearly periodic function for estimating seasonal patterns. Our main effect model, which does not contain any adjustment for season takes $\beta^c(t)$ to be constant across time, i.e.

$$\beta^c(t) = \beta^c. \qquad (2)$$

This model assumes a homogeneous log-linear effect of PM_{10} on mortality, a condition that was found appropriate in previous NMMAPS analyses (9–12).

To allow for different PM_{10} log relative rates by season, we use a pollutant-season interaction model with indicator functions for each season:

$$\beta^c(t) = \beta^c_W\, I_{\text{winter}} + \beta^c_{Sp}\, I_{\text{spring}} + \beta^c_{Sm}\, I_{\text{summer}} + \beta^c_F\, I_{\text{fall}}, \tag{3}$$

where winter, spring, summer, and fall are defined as beginning on December 21st, March 21st, June 21st, and September 21st, respectively. As in model 2, the pollutant-season interaction model assumes a log-linear effect of PM_{10} on mortality, but it provides separate estimates for each season. Although these seasonal estimates serve as concise summaries, it is unlikely that the effect of PM_{10} on mortality is discontinuous across seasons. Furthermore, the estimates depend on the specification of the season boundaries and convey different meanings when this specification changes.

To estimate smooth seasonal patterns in the city-specific log relative rates, we use a sine/cosine model for $\beta^c(t)$ of the form

$$\beta^c(t) = \beta^c_0 + \beta^c_1 \sin(2\pi t/365)/c_1 + \beta^c_2 \cos(2\pi t/365)/c_2 \tag{4}$$

where β^c_0, β^c_{1k}, β^c_{2k} are estimated and c_1 and c_2 are known orthogonalizing constants. In this model, the effect of PM_{10} is allowed to vary smoothly over the course of a year, but is constrained to be periodic across years. While it is possible to include higher frequency basis terms for the representation of $\beta^c(t)$ in equation 4, there is little reason to expect there to be much high frequency variation in the seasonal effects of PM_{10}. Note that the main effect model is nested within the interaction and sine/cosine models, so that if $\beta_W = \beta_{Sp} = \beta_{Sm} = \beta_F$ in equation 3 and $\beta^c_1 = \beta^c_2 = 0$ in equation 4, both models reduce to equation 2.

The potential confounders included in the general model are similar to those used in previous NMMAPS analyses (e.g. 11) and consist of indicators for the day of the week, age specific intercepts corresponding to the categories of less than 65 years of age, 65–74 years, and 75 years or older, a smooth function of calendar time, and smooth functions of temperature and dewpoint temperature. In addition to the overall smooth function of time, two separate smooth functions of time are included for the older two age groups. All of the smooth functions are represented by natural cubic splines.

The complexity of each of the smooth functions of time and temperature is controlled by the numbers of degrees of freedom assigned to each function. We use 7 degrees of freedom per year for the overall smooth function of time, which removes any fluctuations in mortality at time scales longer than two months. The separate smooth functions of time for the older two age categories each receive 1 degree of freedom per year to capture gradual trends specific to these age groups. For temperature we use 6 degrees of freedom and for dewpoint we use 3 degrees of freedom. A somewhat larger number of degrees of freedom is necessary for temperature in order to capture the well known "J-shaped" nonlinear relationship between temperature and mortality. Others have adjusted for temperature simply by doing separate analyses of the data by season (7, 13–17).

All of the above models were fit using standard quasi-likelihood methods implemented in the R statistical software package (18). The software and data are all available on the web at `http://www.ihapss.jhsph.edu`.

Pooling information across cities

After fitting each of the city-specific models we use a hierarchical normal model for pooling information and borrowing strength across cities (see e.g. 15). For a particular model, we have a city-specific maximum likelihood estimate $\widehat{\boldsymbol{\beta}}^c$ which is a scalar for the main effect model in equation 2, a vector of length four for the pollutant-season interaction model in equation 3, and a vector of length three for the sine/cosine model in equation 4. $\widehat{\boldsymbol{\beta}}^c$ is assumed to be normally distributed around the true city-specific log relative rates $\boldsymbol{\beta}^c$ with covariance matrix V^c, estimated within each city. In addition, the true rates are assumed to vary independently across cities according to a normal distribution, i.e.

$$\begin{aligned} \widehat{\boldsymbol{\beta}}^c \mid \boldsymbol{\beta}^c &\sim \mathcal{N}(\boldsymbol{\beta}^c, V^c) \\ \boldsymbol{\beta}^c \mid \boldsymbol{\alpha}, \Sigma &\sim \mathcal{N}(Z^c \boldsymbol{\alpha}, \Sigma) \end{aligned} \tag{5}$$

where Σ is the covariance matrix describing the between-city variation and $\boldsymbol{\alpha}$ is the overall mean for the cities. Z^c is a matrix of second stage covariates for describing possible differences between cities.

To characterize regional differences in seasonal patterns we include as a second stage covariate an indicator for the following seven regions (also used in (7)): Industrial Midwest (19 cities), North East (17), North West (13), Southern California (7), South East (26), South West (10), and Upper Midwest (8).

The final national average estimate $\boldsymbol{\alpha}$ represents the combined information from all of the cities. The diagonal elements of Σ measure the heterogeneity across cities and the off-diagonal elements represent the correlation of the estimates between cities. The hierarchical model is fit using the two level normal independent sampling estimation (TLNise) software of (19) with uniform priors on $\boldsymbol{\alpha}$ and Σ. This software provides a sample from the posterior distribution of Σ from which one can calculate posterior means and variances of the overall and city-specific pollution effects.

Evidence for seasonality in the log relative rates

To quantify the amount of evidence supporting the presence of a seasonal pattern in the national and regional averages we examine the posterior distributions of the pooled log relative rate estimates. In particular, for the sine/cosine model in equation 4, we can check the posterior probability that the coefficients for the harmonic terms are non-zero. While the values of the pooled coefficients β_1 and β_2 do not have meaningful interpretations, if either one of these coefficients is non-zero with high probability, then there is strong evidence of a seasonal trend.

RESULTS

The daily mortality counts for the years 1987–2000 include approximately 10 million deaths. By city, the daily average ranged from 2 deaths per day in Arlington, VA to 190 per day in New York, NY. The daily mean of PM_{10} ranged from 13 $\mu g/m^3$ in Coventry, RI to 49 $\mu g/m^3$ in Fresno, CA. Summary statistics for the dataset are shown in Table 1.

Mortality and PM_{10} levels are known to vary considerably across seasons. With a few exceptions, mortality tends to be higher in the winter and fall and lower in the summer and spring. Figure 1 shows boxplots of the square root daily mortality counts for the largest 10 cities in the United States. Each city shows a clear decrease in mortality towards summer and a peak in the winter. Figure 2 shows the mean daily levels of PM_{10} by season for all cities in each of the seven regions of the U.S. The Southern California, North West, and South West regions have their highest mean levels of PM_{10} in the fall while other regions have their highest levels in the summer.

The national average estimates of the overall and seasonal short-term effects of PM_{10} on mortality for lags 0, 1, and 2 are summarized in Table 2. These estimates were obtained by pooling the city-specific maximum likelihood estimates from the main effect and pollutant-season interaction models according to the hierarchical normal model. Across all seasons, we found that the national average estimate of the effect of PM_{10} on mortality is largest at lag 1 and equal to an estimated 0.19 (95% posterior interval of 0.10, 0.28) percent increase in mortality per 10 μg/m^3 increase in PM_{10}. Previous NMMAPS analyses using data from the eight-year period 1987–1994 have reported similar slightly higher national average estimates for PM_{10} log relative rates (10, 12). For example, the national average estimate reported in (12) was 0.22 (0.03, 0.42).

For PM_{10} at lag 1, the estimates for winter, spring, and fall are similar and equal to 0.15 $(-0.08, 0.39)$, 0.14 $(-0.14, 0.42)$, and 0.14 $(-0.06, 0.34)$, respectively. The estimate for summer is more than twice as large at 0.36 $(0.11, 0.61)$. PM_{10} at lag 0 appears to have a larger effect in the spring and much smaller effects in the other seasons. In addition, estimates for lag 0 have a much larger between season difference (e.g. spring and winter) than those of lag 1. The estimates for lag 2 are generally smaller than those of lag 0 or 1 and, given the size of the posterior intervals, do not vary much across seasons.

Regional differences in the seasonal patterns of the PM_{10} relative rates were explored by including a region indicator variable in the second stage of the hierarchical model. For PM_{10} at lag 1, Figure 3 shows the results of estimating separate seasonal trends from the sine/cosine model for the seven regions of the U.S. The Industrial Midwest and the North East have seasonal trends characterized as being lower in the winter and higher in the summer. Southern California has a larger effect (0.5% per 10 μg/m^3 increase in PM_{10}) that is constant all year. The effect of PM_{10} is close to zero all year round in the North West, South East, South West, and the Upper Midwest, but the North West experiences a slight increase during the summer months. With the exception of Southern California, all regions have a smaller effect in the winter months.

Figure 4 shows samples from the joint posterior distributions of the regionally and nationally pooled harmonic coefficients β_1 and β_2 in the sine/cosine model for PM_{10} at lag 1. The region with the strongest evidence of a seasonal pattern is the North East with a marginal posterior $\text{Prob}(\beta_2 > 0 \mid \text{data}) = 0.94$. There is moderate evidence of seasonality in the Industrial Midwest and the North West with $\text{Prob}(\beta_2 > 0 \mid \text{data}) = 0.83$ and 0.74, respectively. The joint distributions of the coefficients for the South East, South West, Upper Midwest, and Southern California regions are centered at zero, indicating a lack of any seasonal variation. At the national level, the marginal posterior $\text{Prob}(\beta_2 > 0 \mid \text{data}) = 0.91$, while the marginal distribution for β_1 is centered almost exactly around zero. PM_{10} at lag 0 shows slightly more evidence of seasonality for the national average. However, the overall short-term effect of PM_{10} at lag 0 is smaller on average, as indicated in Table 2. There is little evidence of seasonal variation of the short-term effect of PM_{10} at lag 2.

Sensitivity analyses

We performed several additional analyses to explore the sensitivity of the estimated seasonal PM_{10} log relative rates to model specification. Specifically, we examined sensitivity to (1) adjustment for long-term trends and seasonality in mortality; (2) the inclusion of other pollutants; (3) the exposure lag; and (4) the specification of the temperature component.

Estimates of pollution coefficients can change considerably depending on the specification of the number of degrees of freedom in the smooth functions of time to control for long-term trends and seasonality in mortality (note that here we are not referring to the function in equation 4). Our original model used a natural cubic spline with 7 degrees of freedom per year of data. For PM_{10} at lag 1, Figure 5 shows the sensitivity of the sine/cosine model to using 3, 5, 7, 9, and 11 degrees of freedom per year in the smooth function of time. With only 3 degrees of freedom per year the curves deviate considerably from those in Figure 3, e.g. the estimate for Southern

California exhibits much more seasonal variation. However, these deviations more likely reflect a lack of adjustment in the model rather than a real seasonal change. With more aggressive control for seasonality and long-term trends the estimates appear to be stable.

Table 3 shows the sensitivity of the lag 1 PM_{10} log relative rate as other pollutants are included in the pollutant-season interaction model. The seasonal national average estimates exhibit the same pattern when either current day SO_2, O_3, or NO_2 are included as copollutants in the model. With SO_2 included, the summer effect for PM_{10} increases (albeit with increased uncertainty), while the inclusion of O_3 or NO_2 appears to attenuate the effect somewhat. Note that the lack of data for the other pollutants reduced the number of cities available for the copollutant analyses.

Figure 6 shows the region-specific seasonal trends for PM_{10} at lags 0, 1, and 2 with 95% posterior regions for lag 1. The lag 0 seasonal trend for each region has a similar pattern to the lag 1 trend but is lower in general. In the North East and Industrial Midwest, the peak in the seasonal trend for lag 0 appears to come in late May while the peak for lag 1 comes in mid-July. The North West, South East, and Upper Midwest exhibit small changes in seasonal patterns across lags but remain largely flat. Southern California and the South West appear to pick up slightly stronger seasonal patterns in lags 0 and 2.

To explore sensitivity to temperature and to control for temperature effects spread out over multiple days, we fit separate models which included an additional interaction between the current day temperature and the running mean of lags 1 through 3 as well as a running mean of lags 1 through 7. Neither addition to the model made a noticeable impact on the regional or overall seasonal patterns of the PM_{10} log relative rate.

DISCUSSION

In this paper we have used a Bayesian semi-parametric hierarchical model for estimating time-varying effects of air pollution on daily mortality. The model combines information across multiple cities to increase the precision of seasonal relative rate estimates. We found seasonal patterns for the national average effect of PM_{10} at both lag 0 and lag 1. Seasonal patterns varied by geographical region with a strong pattern for lag 1 appearing in the North East region. Equally interesting was the lack of seasonal variation in the southern regions of the country.

Understanding the health effects of PM components is an increasingly important research problem, as noted in (20). Exploration of the spatial-temporal variation of the short-term effects of PM on mortality is essential to generating (or ruling out) specific hypotheses about the toxicity of PM components. Data are becoming available from the Environmental Protection Agency's $PM_{2.5}$ National Chemical Speciation Network which contain detailed time series information on the composition of PM (4). Knowledge of the spatial-temporal patterns of the short-term effects of PM will be necessary for guiding future analyses of these PM constituent data.

The modification of short-term effects of pollution by season has been explored previously in a number of single city studies. Styer, et al. (21) analyzed data from Cook County and Salt Lake County and found (for Cook County) that the effect of PM_{10} was higher in the spring and fall. In a review of research on particulate air pollution and mortality (22), Moolgavkar and Luebeck stated that analyses in Steubenville, Philadelphia, and Cook County indicated that the effects of pollutants are strongly modified by season. Kelsall, et al. (23) examined Philadelphia data and estimated separate pollutant effects by season. They concluded that after adjusting for long-term variation in mortality and the effects of weather there was little evidence of different effects by season. More recently, Moolgavkar (24) analyzed data from Cook County and Los Angeles County and found between season variation of the effects of numerous pollutants on daily mortality in both counties.

Estimation of short-term effects of air pollution on daily mortality for single cities is hampered by the inherent high variability of the resulting effect estimates. Estimation of seasonally varying effects poses an additional challenge because it involves further stratification of the data. Since fewer data are available for estimating season-specific effects, the variability of such estimates increases, making it difficult to discern any meaningful seasonal pattern. Rather, a multi-site approach, where information can be combined across neighboring cities, can provide more precise city-specific log relative rates as well as provide a natural framework for characterizing regional and national trends.

Regional differences in the short-term effects of PM_{10} have been explored in NMMAPS (11, 12) and in the Air Pollution and Health: A European Approach (APHEA) study (25, 26). Both studies found regional modification of the effect of PM_{10} on daily non-accidental mortality. The results presented here are consistent with previous NMMAPS analyses with respect to overall regional average PM_{10} effects. The estimated seasonal patterns for lag 1 appear to have two distinct shapes. The Industrial Midwest, North East, and North West regions all exhibit a larger effect during the summer months while the other regions exhibit little seasonal variation. These patterns are somewhat sensitive to the lag of pollution used. Therefore, an important question raised by this study is how the total effect of PM_{10} in a distributed lags model would vary by season. Unfortunately, the U.S. pollution database has daily PM levels for a small fraction of cities making if difficult to answer this question.

These analyses provide strong evidence that the PM_{10} log relative rate is greater in the spring and summer in the northern regions, particularly in the North East. This result admits several competing hypotheses. First, the PM constituents may vary by season in these regions with the most toxic particles having a spring/summer maximum. A detailed analysis of the regional and seasonal variation in PM constituents is needed to better understand these patterns. Second, even if the constituents do not vary substantially, time spent outdoors tends to be greatest in colder regions during the spring and summer. Hence, the total exposure to particles of outdoor origin may be greatest in these seasons. Third, the particle effect may be swamped by the more powerful effect of winter infectious diseases so that it can only be observed when infectious diseases are less prevalent. This hypothesis does not explain the absence of a PM_{10} mortality association in the southern regions where infectious disease incidence is also seasonal. Finally, this result may reflect seasonally varying bias from an, as yet, unidentified source. Having established the pattern of regional and seasonal variation in the PM_{10} log relative rate, a more targeted investigation of possible sources of such bias is now possible.

References

1. Pope CA, Dockery DW, Schwartz J. Review of epidemiological evidence of health effects of particulate air pollution. Inhalation Toxicology 1995;7:1–18.

2. Dockery DW, Pope CA. Epidemiology of acute health effects: Summary of time-series studies. Wilson R, Spengler J, editors, Particles in Our Air. Harvard University Press, 1996, 123–147.

3. Bell ML, Samet JM, Dominici F. Time-series studies of particulate matter. Annual Review of Public Health 2004;25:247–280.

4. Environmental Protection Agency. Air Quality Criteria for Particulate Matter (Fourth External Review Draft). EPA/600/P-99/002aD and bD. Office of Research and Development, National Center for Environmental Assessment, Research Triangle Park, NC, 2003.

5. Spengler J, Wilson R. Emissions, dispersion, and concentration of particles. Wilson R, Spengler J, editors, Particles in Our Air. Harvard University Press, 1996, 41–62.

6. Environmental Protection Agency. Air Quality Criteria for Particulate Matter. EPA/600/P-95/001aF. Office of Research and Development, Washington DC, 1996.

7. Samet JM, Zeger SL, Dominici F, et al. The National Morbidity, Mortality, and Air Pollution Study (HEI Project No. 96-7): Morbidity and Mortality from Air Pollution in the United States. Health Effects Institute, Cambridge, MA., 2000.

8. Hastie TJ, Tibshirani RJ. Generalized additive models. New York: Chapman and Hall, 1990.

9. Daniels MJ, Dominici F, Samet JM, et al. Estimating particulate matter-mortality dose-response curves and threshold levels: An analysis of daily time-series for the 20 largest us cities. American Journal of Epidemiology 2000;152:397–406.

10. Dominici F, McDermott A, Zeger SL, et al. On the use of generalized additive models in time-series studies of air pollution and health. American Journal of Epidemiology 2002;156:193–203.

11. Dominici F, Daniels M, Zeger SL, et al. Air pollution and mortality: Estimating regional and national dose-response relationships. Journal of the American Statistical Association 2002; 97:100–111.

12. Dominici F, McDermott A, Zeger SL, et al. Mortality among residents of 90 cities. Revised Analysis of the National Morbidity Mortality Air Pollution Study: Part II. The Health Effects Institute, Cambridge, MA, 2003, 9–24.

13. Moolgavkar SH, Luebeck EG, Hall TA, et al. Air pollution and daily mortality in philadelphia. Epidemiology 1995;6:476–484.

14. Samet J, Zeger S, Kelsall J, et al. Does weather confound or modify the association of particulate air pollution with mortality? Environmental Research, Section A 1998;77:9–19.

15. Dominici F, Samet JM, Zeger SL. Combining evidence on air pollution and daily mortality from the twenty largest US cities: A hierarchical modeling strategy (with discussion). Journal of the Royal Statistical Society, Series A 2000;163:263–302.

16. Samet JM, Dominici F, Curriero FC, et al. Fine particulate air pollution and mortality in 20 US cities. New England Journal of Medicine 2000;343:1742–1749.

17. Samet JM, Zeger SL, Dominici F, et al. The National Morbidity, Mortality, and Air Pollution Study (HEI Project No. 96-7): Methods and Methodological Issues. Cambridge, MA: Health Effects Institute., 2000.

18. R Development Core Team. R: A Language and Environment for Statistical Computing. R Foundation for Statistical Computing, Vienna, Austria, 2003. URL `http://www.R-project.org`. ISBN 3-900051-00-3.

19. Everson PJ, Morris CN. Inference for multivariate normal hierarchical models. Journal of the Royal Statistical Society, Series B 2000;62:399–412.

20. National Research Council. Research Priorities for Airborne Particulate Matter: IV. Continuing Research Progress. National Research Council of the National Academies, 2004.

21. Styer P, McMillan N, Gao F, et al. Effect of outdoor airborne particulate matter on daily death counts. Environmental Health Perspectives 1995;103:490–497.

22. Moolgavkar SH, Luebeck EG. A critical review of the evidence on particulate air pollution and mortality. Epidemiology 1996;7:420–428.

23. Kelsall JE, Samet JM, Zeger SL, et al. Air pollution and mortality in Philadelphia, 1974–1988. American Journal of Epidemiology 1997;146:750–762.

24. Moolgavkar SH. Air pollution and daily mortality in two U.S. counties: Season-specific analyses and exposure-response relationships. Inhalation Toxicology 2003;15:877–907.

25. Katsouyanni K, Toulomi G, Samoli E, et al. Confounding and effect modification in the short-term effects of ambient particles on total mortality: Results from 29 european cities within the APHEA2 project. Epidemiology 2001;12:521–513.

26. Samoli E, Schwartz J, Wojtyniak B, et al. Investigating regional differences in short-term effects of air pollution on daily mortality in the APHEA project: A sensitivity analysis for controlling long-term trends and seasonality. Environmental Health Perspectives 2001;109:349–353.

Figures and Tables

	Min.	25%	Median	75%	Max.
Avg. Daily Mortality	2.2	7.6	12.2	20.4	190.2
Avg. Daily PM_{10} ($\mu g/m^3$)	13.2	24.7	27.1	32.0	48.7
Avg. Daily Temp. (° F)	37.0	51.8	58.1	64.7	77.8

Table 1: Summary statistics for average daily mortality, PM_{10}, and temperature for 100 U.S. cities, 1987–2000

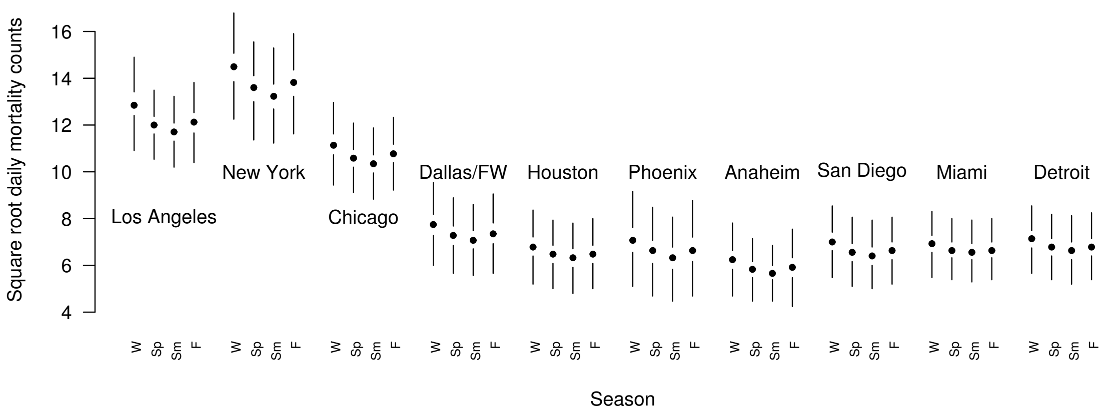

Figure 1: Boxplots of square root daily mortality by season for 10 U.S. cities, 1987–2000.

	Winter	Spring	Summer	Fall	All Seasons
Lag 0	$-0.04_{(-0.30, 0.21)}$	$0.32_{(0.08, 0.56)}$	$0.13_{(-0.11, 0.37)}$	$0.05_{(-0.16, 0.25)}$	$0.09_{(-0.01, 0.19)}$
Lag 1	$0.15_{(-0.08, 0.39)}$	$0.14_{(-0.14, 0.42)}$	$0.36_{(0.11, 0.61)}$	$0.14_{(-0.06, 0.34)}$	$0.19_{(0.10, 0.28)}$
Lag 2	$0.10_{(-0.13, 0.33)}$	$0.05_{(-0.21, 0.32)}$	$-0.03_{(-0.27, 0.21)}$	$0.13_{(-0.08, 0.35)}$	$0.08_{(-0.03, 0.19)}$

Table 2: National average estimates of the overall and seasonal effects of PM_{10} at lags 0, 1, and 2 obtained from the main effect and pollutant-season interaction models (with 95% posterior intervals shown in parentheses). Estimates represent the percent increase in daily mortality for a 10 $\mu g/m^3$ increase in PM_{10}.

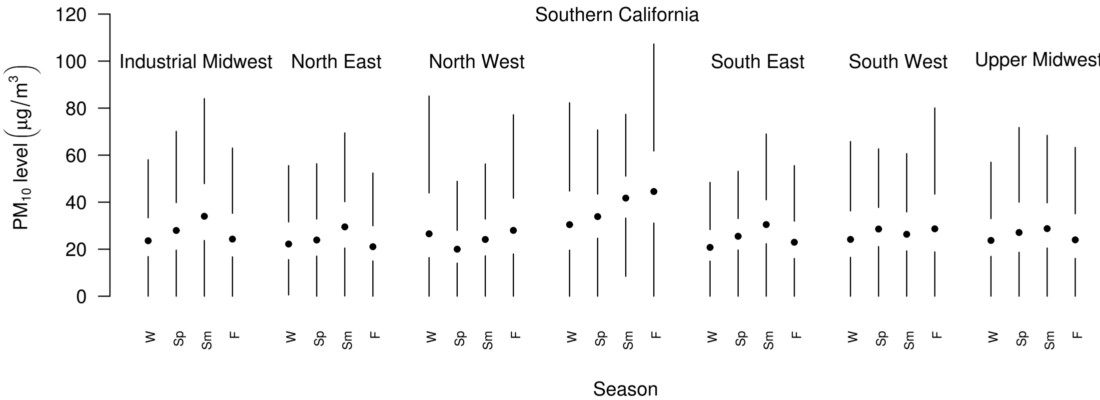

Figure 2: Boxplots of regionally averaged daily PM_{10} levels (in $\mu g/m^3$) by season.

	Winter	Spring	Summer	Fall
PM_{10} only (100 cities)	$0.15_{(-0.08, 0.39)}$	$0.14_{(-0.14, 0.42)}$	$0.36_{(0.11, 0.61)}$	$0.14_{(-0.06, 0.34)}$
with SO_2 (79 cities)	$0.24_{(-0.12, 0.60)}$	$0.05_{(-0.44, 0.55)}$	$0.47_{(-0.04, 0.97)}$	$0.15_{(-0.21, 0.51)}$
with O_3 (72 cities)	$0.21_{(-0.05, 0.47)}$	$0.21_{(-0.08, 0.51)}$	$0.32_{(0.04, 0.59)}$	$0.01_{(-0.28, 0.29)}$
with NO_2 (68 cities)	$0.18_{(-0.15, 0.51)}$	$0.15_{(-0.22, 0.51)}$	$0.34_{(-0.04, 0.72)}$	$0.16_{(-0.18, 0.51)}$

Table 3: Seasonal PM_{10} estimates in two-pollutant models.

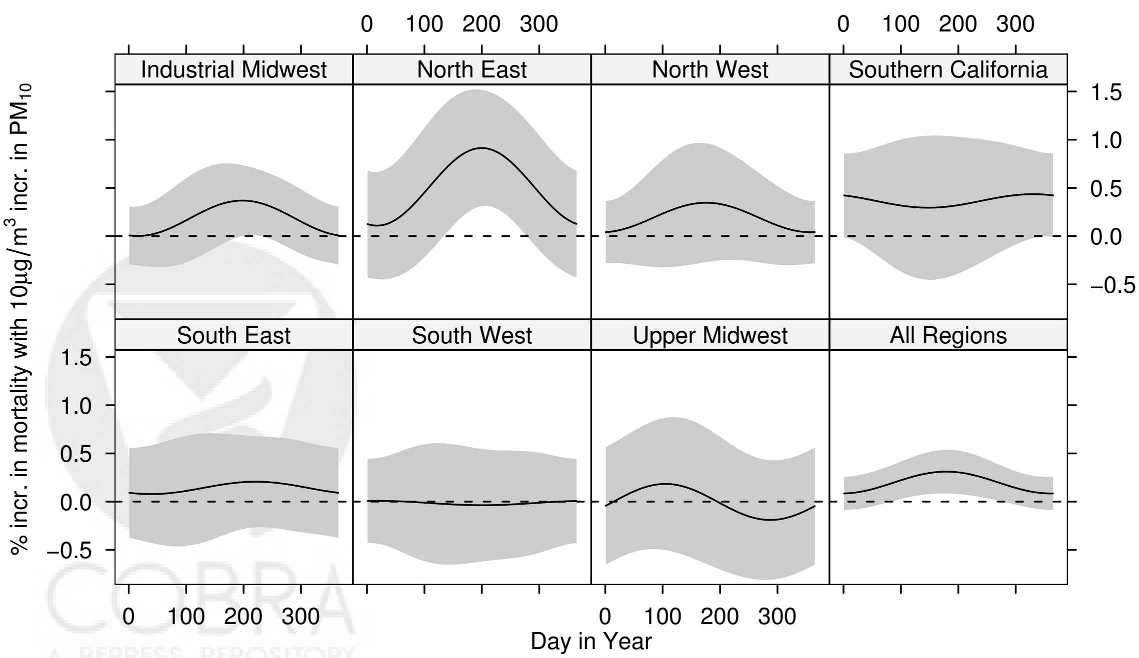

Figure 3: National and regional seasonal curves estimated from the sine/cosine model for lag 1 PM_{10}. Gray regions indicate pointwise 95% posterior intervals.

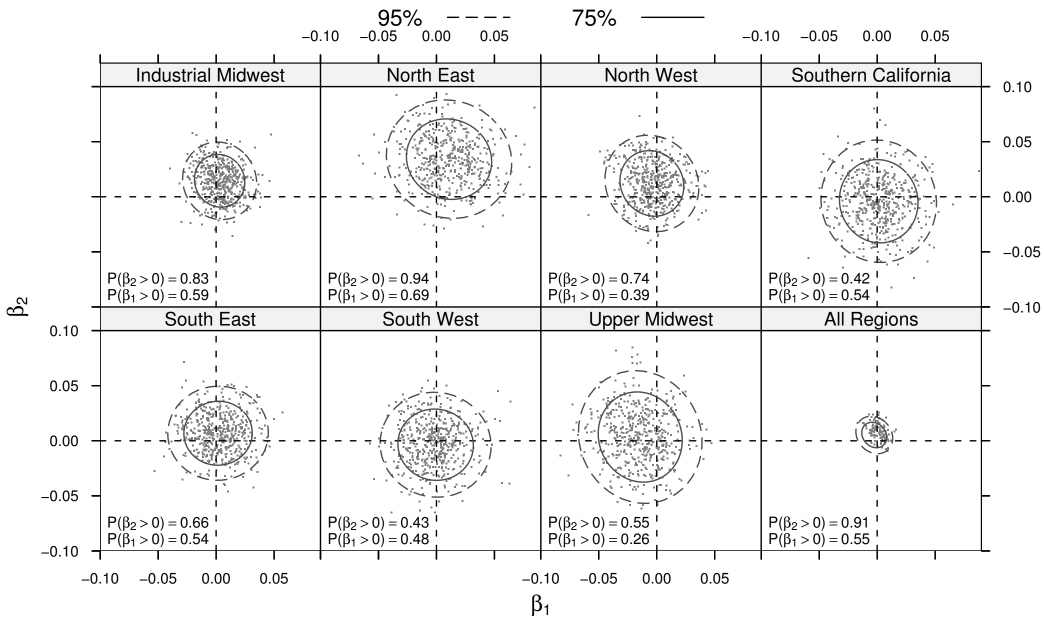

Figure 4: Samples from the national and regional joint posterior distributions of the pooled coefficients β_1 and β_2 from sine/cosine seasonal model for PM_{10} at lag 1. The solid and dashed lines indicate the 75% and 95% regions for the joint posterior distribution of β_1 and β_2, given the data. Noted in each panel are the marginal posterior probabilities of each coefficient being greater than 0.

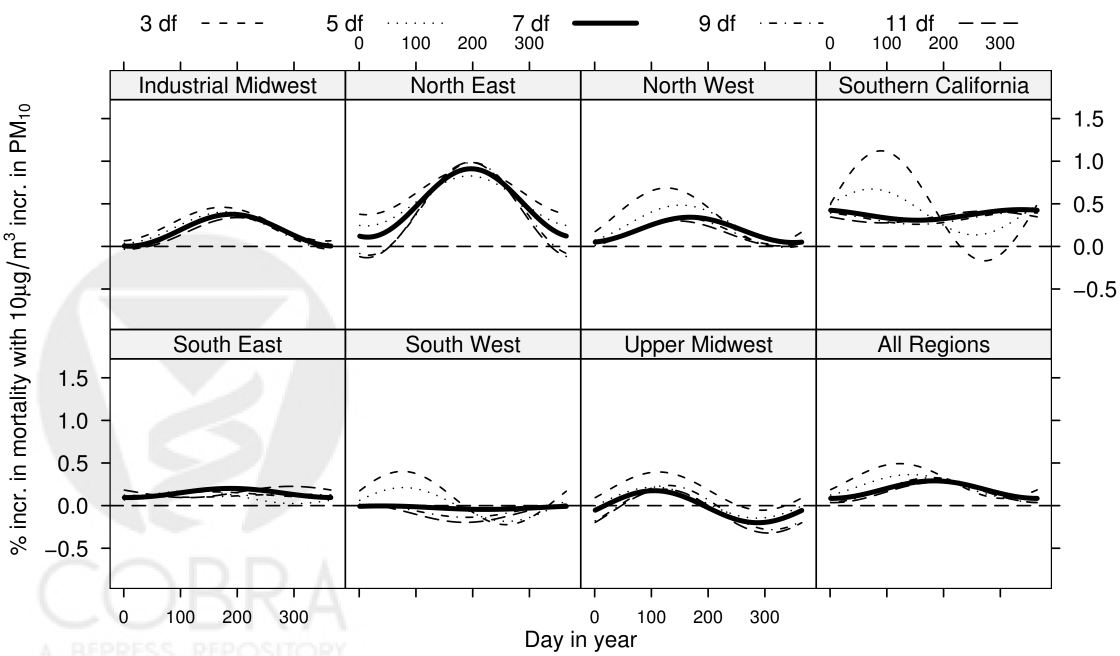

Figure 5: Sensitivity of the sine/cosine model for lag 1 PM_{10} to the degrees of freedom assigned to the smooth function of time.

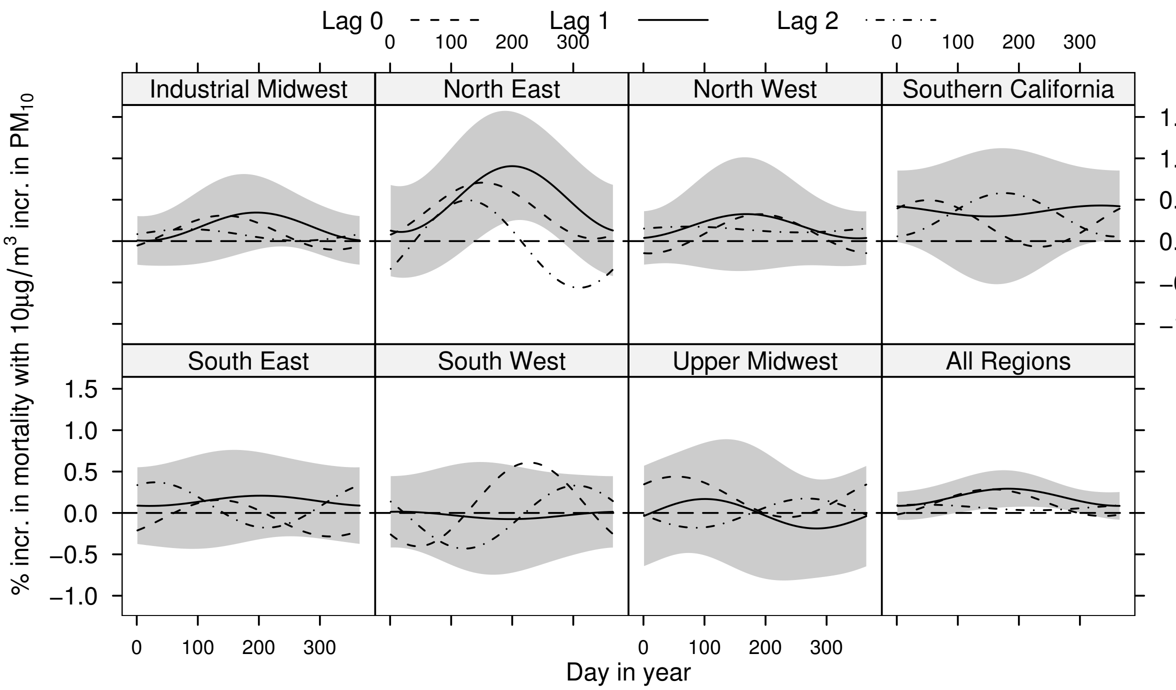

Figure 6: Sensitivity of seasonal patterns to PM_{10} exposure lag in the sine/cosine model. Gray regions indicate pointwise 95% posterior intervals for lag 1.